Pressure ionization in the spherical ion-cell model of dense plasmas and a pressure formula in the relativistic Pauli approximation

Thomas Blenski and Kenichi Ishikawa*
Institut de Génie Atomique, Département de Physique, Ecole Polytechnique Fédérale de Lausanne, CH 1015 Lausanne, Switzerland
(Received 25 July 1994; revised manuscript received 6 December 1994)

We study the continuity of pressure of dense plasmas in the case of pressure ionization. Pressure is calculated using a quantum-mechanical stress-tensor pressure formula in the self-consistent-field spherical ion-cell model. It appears that in order to preserve the continuity of calculated pressure one must take narrow shape resonances into account during the calculations of the self-consistent atomic potential, electron number density, and pressure. We also derive a relativistic pressure formula in the Pauli approximation. The obtained formula is only slightly different from a nonrelativistic one. When there are no very loosely bound levels, relativistic corrections only affect bound electrons, while when very loosely bound levels exist, relativistic corrections to free electron states become important. Hence, if relativistic corrections are applied only to bound electron states, it may lead to a discontinuity in the pressure-versus-density curve even in the case of small-Z elements. This observation stresses the need for a coherent description of bound and free electrons in the spherical ion-cell models.

PACS number(s): 52.25.Jm, 05.70.Ce, 52.25.Kn, 31.30.Jv

I. INTRODUCTION

The self-consistent-field spherical ion-cell model (the ion-sphere model) is often an important part of equation-of-state or opacity calculations of dense plasmas. In the case of strongly coupled plasmas, the dominant electronic contribution to pressure is usually calculated with this model. (See, for instance, Refs. [1–3]).

In some papers using the spherical ion-cell model, bound electrons are treated quantum mechanically, while free electrons are described via the Thomas-Fermi theory [4,5]. More recently, the quantum-mechanical calculations of free-electron density have been proposed and discussed in several papers [6–8]. It is known that a self-consistent field of finite range has continuum resonances accompanying pressure ionization [9]. Several authors (see, for instance, Refs. [9–13]) have studied the disappearance of bound levels and the appearance of resonances and have shown that the transition from bound levels to continuum resonances induces, in principle, no discontinuity in the partition function nor in any thermodynamic quantity within the framework of a spherical-cell central field model. More discussed in Ref. [9] this problem and considered also the problem of pressure calculation. He proposed a quantum-mechanical stress-tensor pressure formula, which could be used in the spherical ion-cell model (see also Ref. [14]).

In the present paper, we generalize the quantum-mechanical stress-tensor pressure formula to the case of relativistic Pauli approximation. The obtained formula differs only slightly from the corresponding expression for the nonrelativistic case. We report some results of our numerical calculations using both nonrelativistic and relativistic formulas. We are especially interested in the problem of the continuity of calculated pressure when pressure ionization takes place. It appears from our calculations that the continuity can be assured only when a careful search for resonances is performed at each step of iterations for the self-consistent atomic potential and when energy integration mesh in calculations of free-electron density takes account of their presence properly.

Our study on the continuity of pressure calculated with relativistic corrections reveals another important observation. Both populations of bound and free electrons should be treated in the same manner, i.e., both with relativistic corrections or both without them. When only bound electrons are treated relativistically and free electrons are considered as nonrelativistic, the total pressure is discontinuous when pressure ionization occurs. This discontinuity appears even in the case where the relativistic corrections to free electrons are expected to be extremely small and where the nonrelativistic treatment of these electrons seems justified. We study the origin of this behavior in detail. It seems that this is an artifact due to the condition of neutrality of the Wigner-Seitz sphere, which is imposed in our spherical ion-cell model. Nevertheless, the discontinuity does not appear when both populations of electrons are calculated in the same way, and the relativistic corrections to free electrons turn out to be small except for the density region where the pressure ionization occurs. Similar effects may appear in other approaches in which bound and free electrons are treated differently.

The present paper is organized as follows. In Sec. II, we recall briefly the spherical ion-cell model and the relativistic corrections to it in the Pauli approximation. The

*Permanent address: Department of Quantum Engineering and Systems Science, Faculty of Engineering, University of Tokyo, Tokyo, Japan.

nonrelativistic stress-tensor pressure formula is presented in Sec. III followed by the derivation of its relativistic version in the Pauli approximation. Section IV presents our results and discussions. We include in this section, also, our results concerning the convergence of free-electron density and pressure with respect to the summation over the azimuthal quantum number l. This question led previously to some controversy in the literature [6–8]. Conclusions are given in Sec. V.

II. ATOMIC MODEL

A. Nonrelativistic spherical ion-cell model

In the nonrelativistic self-consistent spherical ion-cell model, we use the quantum Schrödinger states for free electrons as well as for bound electrons, i.e., the electron number density is obtained by summing over a complete set of bound and free states,

$$n(\mathbf{r})=\sum_i |\Psi_i(\mathbf{r})|^2 f(\varepsilon_i,\mu) , \tag{2.1}$$

where, f is the Fermi-Dirac function:

$$f(\varepsilon,\mu)=\left[\exp\left[\frac{\varepsilon-\mu}{T}\right]+1\right]^{-1} . \tag{2.2}$$

The wave functions are calculated from the radial Schrödinger equation:

$$\left[-\frac{\hbar^2}{2m}\left[\frac{2^2}{dr^2}-\frac{l(l+1)}{r^2}\right]-eV_{\rm sc}\right]y_{\varepsilon,l}(r)=\varepsilon y_{\varepsilon,l}(r) , \tag{2.3}$$

$$\Psi_i(\mathbf{r})=\frac{y_{\varepsilon,l}(r)}{r}Y_{lm}(\theta,\varphi) , \tag{2.4}$$

where $Y_{lm}(\theta,\varphi)$ is a spherical harmonic. Bound states are found using the phase function method, which is described elsewhere [15]. The self-consistent potential $V_{\rm sc}(\mathbf{r})$ is

$$-eV_{\rm sc}(\mathbf{r})=-eV_{\rm el}(\mathbf{r})+V_{\rm xc}(\mathbf{r}) , \tag{2.5}$$

where $e(>0)$ is an absolute value of the electronic charge, and $V_{\rm el}(\mathbf{r})$ is the electrostatic potential, which is determined by the electron and nuclear charges via the Poisson equation:

$$\nabla^2 eV_{\rm el}(\mathbf{r})=\frac{e^2}{\varepsilon_0}n(\mathbf{r}) , \tag{2.6}$$

where ε_0 is the permittivity of vacuum, with the boundary conditions,

$$eV_{\rm el}(\mathbf{r})\underset{r\to 0}{\sim}\frac{1}{4\pi\varepsilon_0}\frac{Ze^2}{r} , \tag{2.7}$$

$$V_{\rm sc}(r)=0 , \frac{dV_{\rm el}}{dr}(r)=0 \quad \text{on } r\geq r_0 , \tag{2.8}$$

with r_0 being the radius of the Wigner-Seitz sphere defined by

$$r_0=\left[\frac{3}{4\pi\rho}\right]^{1/3} , \tag{2.9}$$

where ρ indicates the number density of atoms. In Eq. (2.5) $V_{\rm xc}(\mathbf{r})$ is the exchange-correlation potential, for which, in practical calculations, we use formulas given in Ref. [16]. (See also Ref. [17].) In the first of Eq. (2.8), we assume that the self-consistent potential is constant for $r\geq r_0$ and set this constant equal to zero. This assumption requires that the total electron density, determined from Eq. (2.1), is also nearly constant and equal to its asymptotic value for $r\to\infty$. The charge neutrality outside the Wigner-Seitz sphere is assumed to be assured by a constant homogeneous positive ion distribution. Since we use the local density approximation, the exchange-correlation potential $V_{\rm xc}(r)=V_{\rm xc}(n(r))$ is also assumed to be constant for $r\geq r_0$. The first Eq. (2.8) can, therefore, be seen as the condition $eV_{\rm el}(r_0)=V_{\rm xc}(n(r_0))$. The second of Eq. (2.8) is required by the neutrality condition within the Wigner-Seitz sphere, from which the chemical potential μ is found. We will return to the problem of the constant electronic density for $r\geq r_0$ in Sec. IV C.

B. Relativistic corrections

We use the Pauli theory [18], in which only first-order relativistic corrections to the Schrödinger equation are retained. This approximation is sufficient for most of practical problems. The Pauli theory gives an approximate equation for the large components U_A of Dirac spinor. For a central potential, the radial part $y(r)$ of U_A satisfies the following wave equation:

$$\left[-\frac{\hbar^2}{2m}\left[\frac{d^2}{dr^2}-\frac{l(l+1)}{r^2}\right]-eV_{\rm sc}+V_{\rm mv}+V_{\rm Darwin}+V_{\rm so}\right]y(r)=\varepsilon y(r) . \tag{2.10}$$

Compared with the Schrödinger equation (2.3), this equation has three additional terms, i.e., the mass-velocity term $V_{\rm mv}$, the Darwin term $V_{\rm Darwin}$, and the spin-orbit term $V_{\rm so}$:

$$V_{\rm mv}=-\frac{(\varepsilon+eV_{\rm sc})^2}{2E_0} , \tag{2.11}$$

$$V_{\rm Darwin}=\frac{\hbar^2}{2m}\frac{1}{2E_0+\varepsilon+eV_{\rm sc}}e\frac{dV_{\rm sc}}{dr}\left[\frac{d}{dr}-\frac{1}{r}\right] , \tag{2.12}$$

$$V_{\rm so}=-\frac{\hbar^2}{2m}\frac{1}{2E_0+\varepsilon+eV_{\rm sc}}e\frac{dV_{\rm sc}}{dr}\frac{X}{r} , \tag{2.13}$$

where X is an eigenvalue of the operator $2\mathbf{L}\cdot\mathbf{s}$, and E_0 is the rest-mass energy of electron. In the original version of the Pauli theory, the expression $(2E_0+\varepsilon+eV_{\rm sc})^{-1}$ in Eqs. (2.12) and (2.13) is replaced by $(2E_0)^{-1}$. We use, however, the present version of these equations for the reason described in Ref. [19]. Since the effect of the Darwin term is small in the case of $l\geq 1$ [19], we omit this term for $l\geq 1$ in practical calculations. We replace X

by its average value $\bar{X}=0$ (see Appendix A). The angular dependence of U_A is summarized in Appendix A.

C. Calculation of the electron density

In the case of a central potential, the radial wave function $y_{\varepsilon,l}(r)$ is normalized as follows:

$$\int_0^\infty dr y_{\varepsilon_a,l}(r)y_{\varepsilon_b,l}(r)=\begin{cases}\delta_{a,b} & \text{for bound states}\\ \delta(\varepsilon_a-\varepsilon_b) & \text{for free states .}\end{cases} \tag{2.14}$$

As the potential is constant outside the ion sphere, the radial wave function of bound states outside the sphere can be written as

$$y_{nl}(r)=\begin{cases}C_{nl}r\kappa_l(-ikr) & \text{for the nonrelativistic model}\\ C_{nl}r\kappa_l(-iKr) & \text{for the relativistic model ,}\end{cases} \tag{2.15}$$

where κ_l is the modified spherical Bessel function of the third kind [20] k and K are defined as

$$k=\left[\frac{2m\varepsilon}{\hbar^2}\right]^{1/2},\quad K=\left[\frac{2m\varepsilon}{\hbar^2}\left[1+\frac{\varepsilon}{2E_0}\right]\right]^{1/2}, \tag{2.16}$$

and $C_{n,l}$ is a constant determined by the normalization and by the boundary conditions at r_0. As follows from Eq. (2.8) the bound-electron wave functions extend beyond r_0. The condition that their logarithmic derivatives are continuous at r_0 determines the one-electron eigenvalues ε. The radial wave function of a free state outside the ion-sphere can be written as

$$y_{\varepsilon,l}(r)=\begin{cases}\left[\frac{2m}{\hbar^2}\frac{k}{\pi}\right]^{1/2} r[\cos\delta_{\varepsilon,l}j_l(kr)-\sin\delta_{\varepsilon,l}n_l(kr)] & \text{for the nonrelativistic model}\\ \left[\frac{2m}{\hbar^2}\frac{K}{\pi}\right]^{1/2}\left[1+\frac{\varepsilon}{E_0}\right]r[\cos\delta_{\varepsilon,l}j_l(Kr)-\sin\delta_{\varepsilon,l}n_l(Kr)] & \text{for the relativistic model ,}\end{cases} \tag{2.17}$$

where j_l and n_l denote spherical Bessel functions of the first and the second kinds [20], respectively, and $\delta_{\varepsilon,l}$ is the phase shift. k and K are pure imaginary for bound levels and real for free levels.

With the normalization (2.14), the electron number density (2.1) can be written in terms of the radial wave functions as follows:

$$n(\mathbf{r})=n_{\text{bound}}(\mathbf{r})+n_{\text{free}}(\mathbf{r}) , \tag{2.18}$$

$$n_{\text{bound}}(\mathbf{r})=\sum_{n,l\in\text{bound}} f(\varepsilon_{nl},\mu)\frac{2(2l+1)}{4\pi}\frac{y_{nl}^2(r)}{r^2} , \tag{2.19}$$

$$n_{\text{free}}(\mathbf{r})=\int_0^\infty d\varepsilon f(\varepsilon,\mu)\sum_{l=0}^{\infty}\frac{2(2l+1)}{4\pi}\frac{y_{\varepsilon,l}^2(r)}{r^2} . \tag{2.20}$$

The neutrality condition of the Wigner-Seitz sphere [Eqs. (2.8) and (2.9)] involves the bound and free wave functions only for $r\le r_0$. In numerical calculations, we sum in Eq. (2.20) over only a few values of $l\le l_{\max}$. In performing this summation, rather than summing up to $l_{\max}$ directly, i.e.,

$$n_{\text{free}}(\mathbf{r})\cong\int_0^\infty d\varepsilon(\varepsilon,\mu)\sum_{l=0}^{l_{\max}}\frac{2(2l+1)}{4\pi}\frac{y_{\varepsilon,l}^2(r)}{r^2} , \tag{2.21}$$

it is better to divide Eq. (2.21) into two parts as follows [7,8]:

$$n_{\text{free}}(\mathbf{r})\cong\int_0^\infty d\varepsilon f(\varepsilon,\mu)\times\left[\sum_{l=0}^{l_{\max}}\frac{2(2l+1)}{4\pi}\frac{y_{\varepsilon,l}^2(r)-y_{0;\varepsilon,l}^2(r)}{r^2}+\sum_{l=0}^{\infty}\frac{2(2l+1)}{4\pi}\frac{y_{0;\varepsilon,l}^2(r)}{r^2}\right] , \tag{2.22}$$

where the subscript 0 indicates the normalized radial wave functions of the case where there is no potential, which can be obtained by setting $\delta_{\varepsilon,l}=0$ in Eq. (2.17). In Eq. (2.22) we have used the fact that the phase shift $\delta_{\varepsilon,l}$ rapidly tends to zero as l increases and that at $l>l_{\max}$, the radial wave function $y_{\varepsilon,l}$ is very close to $y_{0;\varepsilon,l}$. The second term of the integrand (the homogeneous part) can be calculated analytically using Eq. (2.17) and the identity $\sum_{l=0}^{\infty}(2l+1)j_l^2(x)=1$ [20]:

$$\sum_{l=0}^{\infty}\frac{2(2l+1)}{4\pi}\frac{y_{0;\varepsilon,l}(r)}{r^2}=\begin{cases}\frac{2m}{\hbar^2}\frac{k}{2\pi^2} & \text{(the nonrelativistic model)}\\ \frac{2m}{\hbar^2}\frac{K}{2\pi^2}\left[1+\frac{\varepsilon}{E_0}\right]^2 & \text{(the relativistic model).}\end{cases} \tag{2.23}$$

As shown later, retaining $l_{\max}=10$ leads to sufficient accuracy with Eq. (2.22), while $l_{\max}$ as much as 40 or 50 is needed for the direct summation formula, Eq. (2.21).

D. Method of search for resonances

As is well known [9], a finite-range potential may have continuum resonances. In the nonrelativistic model, the derivative of the phase shift with respect to the wave number, $d\delta_l/dk$ can be expressed in terms of the complex resonance wave number $Q_{n,l}$ [9]:

$$\frac{d\delta_l}{dk}=2\sum_{n>0}\mathrm{Im}\left[\frac{k^2}{Q_{n,l}(k^2-Q_{n,l}^2)}\right], \tag{2.24}$$

where $l\geq 1$, since there are no resonances for $l=0$ [9]. Generally, $Q_{n,l}$ is a complex number and can be written as,

$$Q_{n,l}=\kappa_{n,l}+i\gamma_{n,l}, Q_{-n,l}=-\kappa_{n,l}+i\gamma_{n,l} \quad (n>0,\ \kappa_{n,l},\gamma_{n,l}\geq 0). \tag{2.25}$$

Substituting Eq. (2.25) into (2.24), we obtain

$$\frac{d\delta_l}{dk}=2k^2\sum_{n>0}\frac{\gamma_{n,l}}{\kappa_{n,l}^2+\gamma_{n,l}^2}\times\frac{3\kappa_{n,l}^2-\gamma_{n,l}^2-k^2}{[k^2-(\kappa_{n,l}^2-\gamma_{n,l}^2)]^2+(2\kappa_{n,l}\gamma_{n,l})^2}. \tag{2.26}$$

If $\gamma_{n,l}$ is much smaller than $\kappa_{n,l}$, the resonance associated with that complex resonance wave number appears in the continuum. When $k\cong\kappa_{n,l}\gg\gamma_{n,l}$, the contribution of all the other complex resonance wave numbers can be neglected, and we obtain

$$\frac{d\delta_l}{dk}\cong\frac{\gamma_{n,l}}{(k-\kappa_{n,l})^2+\gamma_{n,l}^2} \tag{2.27}$$

and

$$\frac{d\delta_l}{d\varepsilon}\cong\frac{\Gamma_{n,l}}{(\varepsilon-\varepsilon_{n,l})^2+\Gamma_{n,l}^2}, \tag{2.28}$$

where $\varepsilon_{n,l}=\hbar^2\kappa_{n,l}^2/2m$ and $\Gamma_{n,l}=\hbar^2\kappa_{n,l}\gamma_{n,l}/m$. Equations (2.27) and (2.28) indicate that the phase shift increases abruptly near the resonances position. Therefore, the resonance can be found as the (real) wave number $k=\kappa_{n,l}$ such that (see also Ref. [21])

$$\frac{d^2\delta_l}{dk^2}=0 \quad\text{and}\quad \frac{d\delta_l}{dk}>0, \tag{2.29}$$

and the half width $\gamma_{n,l}$ of the resonance is given by

$$\gamma_{n,l}=\left[\left(\frac{d\delta_l}{dk}\right)_{k=\kappa_{n,l}}\right]^{-1}, \tag{2.30}$$

Although Eqs. (2.24) and (2.26) do not apply strictly in the relativistic (Pauli) model, we can find resonances in the same way, i.e., using Eqs. (2.29) and (2.30).

III. PRESSURE FORMULA

A. Nonrelativistic stress-tensor pressure formula

The nonrelativistic quantum-mechanical stress tensor (momentum tensor) P_{ij} is defined as follows [9,22]:

$$P_{ij}(\mathbf{r})=\frac{\hbar^2}{2m}\sum_s f(\varepsilon_s,\mu)\mathrm{Re}\left[\frac{\partial\psi_s^*}{\partial x_i}\frac{\partial\psi_s}{\partial x_j}-\psi_s^*\frac{\partial^2\psi_s}{\partial x_i\partial x_j}\right]+\delta_{ij}P_{\mathrm{xc}}(\mathbf{r}), \tag{3.1}$$

$$P_{\mathrm{xc}}(\mathbf{r})=-\int_0^{n(\mathbf{r})}V_{\mathrm{xc}}(n')dn'+V_{\mathrm{xc}}(n)n(\mathbf{r}). \tag{3.2}$$

It seems reasonable [9] to calculate the pressure by evaluating the radial stress P_{rr} at the radius of the ion-sphere r_0. Then the pressure is given by

$$P_{\mathrm{total}}=\frac{\hbar^2}{2m}\sum_{\varepsilon,l}\frac{2(2l+1)}{4\pi}f(\varepsilon,\mu)\times\left[\left(\frac{d}{dr}\frac{y_{\varepsilon,l}}{r}\right)^2-\frac{y_{\varepsilon,l}}{r}\frac{d^2}{dr^2}\left[\frac{y_{\varepsilon,l}}{r}\right]\right]_{r=r_0}+P_{\mathrm{xc}}(r_0). \tag{3.3}$$

As $V_{\mathrm{sc}}(r_0)=0$, the pressure P_{total} can be written in the form:

$$P_{\mathrm{total}}=P_{\mathrm{bound}}+P_{\mathrm{free}}+P_{\mathrm{xc}}. \tag{3.4}$$

with

$$P_{\mathrm{bound}}=\sum_{n,l\in\mathrm{bound}}f(\varepsilon_{nl},\mu)\Pi_{k,l}(y_{nl}), \tag{3.5}$$

$$P_{\mathrm{free}}=\int_0^\infty d\varepsilon f(\varepsilon,\mu)\sum_{l=0}^{\infty}\Pi_{k,l}(y_{\varepsilon,l}), \tag{3.6}$$

where Π is defined as

$$\Pi_{k,l}(y(r))=\frac{\hbar^2}{2m}\frac{2(2l+1)}{4\pi r_0^2}\times\left[\left[\frac{dy}{dr}\right]_{r_0}^2+\left[k^2-\frac{l^2+l+1}{r_0^2}\right][y(r_0)]^2\right]. \tag{3.7}$$

Bound-electron pressure P_{bound} and exchange-correlation pressure P_{xc} are always negative. Generally only the contributions of loosely bound levels are important while those of tightly bound levels are extremely small. In free-electron pressure P_{free}, the pressure of low-energy free electrons is slightly negative, and that of high-energy free electrons is significantly positive. The resonance pressure, which is attributed to the additional density of states due to narrow resonances, is included in P_{free}. The pressure of a narrow resonance is important and negative. In principle, the thermal ionic contribution should be included in pressure calculations [3]. It is neglected in the present study since we consider mainly strongly coupled plasmas.

B. Relativistic pressure formula in the Pauli approximation

We start with the Dirac equation:

$$[-eV_{\mathrm{sc}}+\beta E_0+c\boldsymbol{\alpha}\cdot\mathbf{p}]\Psi_s=E_s\Psi_s, \tag{3.8}$$

and the relativistic stress-strain tensor (energy-momentum tensor) $\mathbf{P}$ [22],

$$P_{ij}(\mathbf{r})=c\hbar\sum_s f(\varepsilon_s,\mu)\mathrm{Im}\left[\Psi_s^+\alpha_j\frac{\partial\Psi_s}{\partial x_i}\right]+\delta_{ij}P_{\mathrm{xc}}(\mathbf{r}) , \tag{3.9}$$

where $\varepsilon_s=E_s-E_0$, Ψ_s is the Dirac spinor and α_i and β are the Dirac matrices. In Eq. (3.9) the exchange-correlation pressure P_{xc} is given by Eq. (3.2). We calculate the pressure again by evaluating the radial stress P_{rr} at $r=r_0$:

$$P_{\mathrm{total}}=c\hbar\sum_s f(\varepsilon_s,\mu)\mathrm{Im}\left[\Psi_s^+\hat{\mathbf{r}}\cdot\boldsymbol{\alpha}\frac{\partial\Psi_s}{\partial r}\right]_{r=r_0}+P_{\mathrm{xc}}(r_0) , \tag{3.10}$$

where $\hat{\mathbf{r}}=\mathbf{r}/r$.

Now, we show that the Pauli approximation to the Dirac theory reduces the relativistic pressure formula, Eq. (3.10) to a form similar to the nonrelativistic one, Eq. (3.3). The large components U_A and the small components U_B of Ψ_s satisfy the following relationship [18]:

$$U_B=\frac{c\sigma^p\cdot\mathbf{p}}{E_s+E_0+eV_{\mathrm{sc}}}U_A , \tag{3.11}$$

where σ^p is the Pauli (two-by-two) spin matrices. Then $\alpha\Psi_s$ can be written in terms of U_A [18]:

$$\alpha\Psi_s=\begin{bmatrix}\dfrac{c}{E_s+E_0+eV_{\mathrm{sc}}}\{\mathbf{p}+i(\mathbf{p}\times\sigma^p)\}U_A\\ \sigma^pU_A\end{bmatrix} . \tag{3.12}$$

Using Eqs. (3.11) and (3.12), one gets,

$$\begin{aligned}\Psi_s^+\hat{\mathbf{r}}\cdot\boldsymbol{\alpha}\frac{\partial\Psi_s}{\partial r}=(\hat{\mathbf{r}}\cdot\boldsymbol{\alpha}\Psi_s)^+\frac{\partial\Psi_s}{\partial r}=\frac{ic\hbar}{E_s+E_0+eV_{\mathrm{sc}}}\Bigg[&\left[\frac{\partial U_A^+}{\partial r}\frac{\partial U_A}{\partial r}-U_A^+\frac{\partial^2U_A}{\partial r^2}\right]\\&-2\left\{\frac{(\mathbf{L}\cdot\mathbf{s}U_a)^+}{r}\frac{\partial U_A}{\partial r}-U_A^+\frac{\partial}{\partial r}\left[\frac{\mathbf{L}\cdot\mathbf{s}U_A}{r}\right]\right\}\\&-U_A^+\frac{e}{E_s+E_0+eV_{\mathrm{sc}}}\frac{\partial V_{\mathrm{sc}}}{\partial r}\left[-\frac{\partial}{\partial r}+\frac{2\mathbf{L}\cdot\mathbf{s}}{r}\right]U_A\Bigg] ,\end{aligned} \tag{3.13}$$

where we have used the following identities [23], [18]:

$$(\sigma^p\cdot\mathbf{A})(\sigma^p\cdot\mathbf{B})=\mathbf{A}\cdot\mathbf{B}+i\sigma^p\cdot(\mathbf{A}\times\mathbf{B}) , \tag{3.14}$$

$$s=\sigma^p/2 . \tag{3.15}$$

The discussion so far is rigorous. In this stage, we introduce the Pauli approximation. In this approximation, since U_A is the eigenstate of $2\mathbf{L}\cdot\mathbf{s}$ with the eigenvalue X, we obtain

$$\begin{aligned}\Psi_s^+\hat{\mathbf{r}}\cdot\boldsymbol{\alpha}\frac{\partial\Psi_s}{\partial r}=\frac{ic\hbar}{E_s+E_0+eV_{\mathrm{sc}}}\Bigg[&\left[\frac{\partial U_A^+}{\partial r}\frac{\partial U_A}{\partial r}-U_A^+\frac{\partial^2U_A}{\partial r^2}\right]-\frac{XU_A^+U_A}{r^2}\\&-\frac{e}{E_s+E_0+eV_{\mathrm{sc}}}\frac{\partial V_{\mathrm{sc}}}{\partial r}\left[-U_A^+\frac{\partial U_A}{\partial r}+\frac{XU_A^+U_A}{r}\right]\Bigg] .\end{aligned} \tag{3.16}$$

As described in Appendix A, there are $2(2l+1)$ states for given ε (or n) and l. In the present study, since we set $V_{\mathrm{so}}=0$ in Eq. (2.10), the radial wave function $y_{\varepsilon,l}(r)$ is common to all these states. If we assume that these states are equally populated by electrons and use Eq. (A7), we get the radial stress as follows:

$$\begin{aligned}P_{rr}(r)-P_{\mathrm{xc}}(r)=\frac{\hbar^2}{2m}\sum_{\varepsilon,l}\frac{2(2l+1)}{r\pi}\frac{2E_0}{2E_0+\varepsilon+eV_{\mathrm{sc}}}f(\varepsilon,\mu)\\\times\left[\left[\frac{d}{dr}\frac{y_{\varepsilon,l}}{r}\right]^2-\frac{y_{\varepsilon,l}}{r}\frac{d^2}{dr^2}\left[\frac{y_{\varepsilon,l}}{r}\right]+\frac{e}{2E_0+\varepsilon+eV_{\mathrm{sc}}}\frac{\partial V_{\mathrm{sc}}}{\partial r}\frac{y_{\varepsilon,l}}{r}\frac{d}{dr}\frac{y_{\varepsilon,l}}{r}\right] .\end{aligned} \tag{3.17}$$

It finally follows, since $V_{sc}(r_0)=0$ and $\partial V_{sc}/\partial r(r_0)=0$, that the pressure formula in the Pauli approximation is

$$P_{\text{total}}=\frac{\hbar^2}{2m}\sum_{\varepsilon,l}\frac{2(2l+1)}{4\pi}\frac{1}{1+\varepsilon/2E_0}f(\varepsilon,\mu) \times\left[\left[\frac{d}{dr}\frac{y_{\varepsilon,l}}{r}\right]^2-\frac{y_{\varepsilon,l}}{r}\frac{d^2}{dr^2}\left[\frac{y_{\varepsilon,l}}{r}\right]\right]_{r=r_0} +P_{\text{xc}}(r_0) \tag{3.18}$$

$$=P_{\text{bound}}+P_{\text{free}}+P_{\text{xc}}\ , \tag{3.19}$$

$$P_{\text{bound}}=\sum_{n,l\in\text{bound}}\frac{f(\varepsilon_{nl},\mu)}{1+\varepsilon_{nl}/2E_0}\Pi_{K,l}(y_{nl})\ , \tag{3.20}$$

$$P_{\text{free}}=\int_0^\infty d\varepsilon\frac{f(\varepsilon,\mu)}{1+\varepsilon/2E_0}\sum_{l=0}^{\infty}\Pi_{K,l}(y_{\varepsilon,l})\ . \tag{3.21}$$

The obtained formula, Eq. (3.18) is different from the nonrelativistic formula, Eq. (3.3) only by the factor $(1+\varepsilon/2E_0)^{-1}$, which is close to unity. Thus, we have found that the Pauli theory for a central potential reduces the relativistic pressure formula to the form which is similar to the nonrelativistic one.

C. Calculation of P_{free}

To obtain free-electron pressure P_{free} according to Eq. (3.6) or (3.21) in numerical calculations, we approximate $\sum_{l=0}^{\infty}\Pi_{k\text{ or }K,l}(y_{\varepsilon,l})$ by summing over $0\le l\le l_{\max}$ either by a direct summation,

$$\sum_{l=0}^{\infty}\Pi_{k,l}(y_{\varepsilon,l})\cong\sum_{l=0}^{l_{\max}}\Pi_{k,l}(y_{\varepsilon,l})\ , \tag{3.22}$$

or by the separation of the homogeneous part,

$$\sum_{l=0}^{\infty}\Pi_{kl}(y_{\varepsilon,l})\cong\sum_{l=0}^{l_{\max}}\{\Pi_{k,l}(y_{\varepsilon,l})-\Pi_{k,l}(y_{0;\varepsilon,l})\} +\sum_{l=0}^{\infty}\Pi_{k,l}(y_{0;\varepsilon,l})\ . \tag{3.23}$$

In the relativistic formula, k's must be replaced by K's. The second term of the right hand side (rhs) (the homogeneous part) of Eq. (3.23) can be calculated analytically (See Appendix B):

$$\sum_{l=0}^{\infty}\Pi_{k,l}(y_{0;\varepsilon,l})=\frac{k^3}{3\pi^2}\quad\text{for the nonrelativistic treatment}\ ,$$
$$\sum_{l=0}^{\infty}\Pi_{k,l}(y_{0;\varepsilon,l})=\frac{K^3}{3\pi^2}\left[1+\frac{\varepsilon}{E_0}\right]^2\quad\text{for the relativistic treatment}\ . \tag{3.24}$$

Similarly as in the calculation of free-electron density n_{free}, Eq. (3.23) is more efficient than Eq. (3.22).

IV. RESULTS AND DISCUSSIONS

A. Convergence with respect to l

First, we discuss the convergence with respect to the azimuthal quantum number l. This problem appears both in self-consistent calculations of atomic potential and electron density, and in calculations of pressure. In both cases the homogeneous part can be separated and calculated analytically, which reduces the cut value $l_{\max}$ needed for convergence [compare Eqs. (2.21) and (2.22) for free-electron density and Eqs. (3.22) and (3.23) for free-electron pressure]. In one of the first papers in which the free-electron density was calculated via wave functions, Davis and Blaha [6], who did not use the above mentioned separation, reported that large values of $l_{\max}$ (50 or 70) were necessary. Dharma-wardana and Perrot [7] introduced the separation and retained $l_{\max}$ equal to 8 or 10. More recently, Beynon and Landeg [8] found that $l_{\max}=3$ was sufficient in the case of aluminum at 30-eV temperature and at 0.4 of solid density.

In Table I, we show the one-electron bound energy levels of iron at 200-eV temperature and 0.1 solid density obtained using relativistic formulas, Eqs. (2.10)–(2.13) with different values of $l_{\max}$. We present results calculated using Eqs. (2.21) and (3.22) (without the separation into the homogeneous and nonhomogeneous parts) and with Eqs. (2.22) and (3.23) (with the separation). We give the number of free electrons contained inside the ion sphere in the second row from the bottom and the total pressure in the last row. It seems that a good convergence is obtained by taking $l_{\max}=50$ in calculations without the separation and $l_{\max}=20$ with the separation although in the latter case $l_{\max}=10$ gives already good accuracy. We have found that in plasmas of higher densities and lower temperatures than in our example in Table I, $l_{\max}=10$ leads to relatively good convergence when Eqs. (2.22) and (3.23) are used. However for higher temperatures and lower densities than in our example, higher value of $l_{\max}$ may sometimes be necessary even when Eq. (2.22) and (3.23) are applied. All the results of our calculations presented in what follows were performed with the separation into the homogeneous and nonhomogeneous parts and with $l_{\max}=10$.

B. Comparison with other calculations and experimental results for zero-temperature case

Figure 1 presents results of our calculations and those obtained by Young, Wolford, and Rogers [24], for aluminum at zero temperature. In Fig. 2, the comparison of

TABLE I. The one-electron bound energy levels of Fe plasma at $T=200$ eV and $\rho=0.1\rho_0$ ($\rho_0=7.86$ g/cm^3). All the energy values are in eV and minus signs are omitted. The second row from the bottom is the number of free electrons contained inside the Wigner-Seitz sphere. The last row is the total pressure in Mbar. The numbers in brackets denote multiplicative powers of ten.

		Without the separation Eqs. (2.21) and (3.22)			With the separation Eqs. (2.22) and (3.23)		
Level	$l_{max}20$	30	40	50	10	20	50
1s	6.79 [3]	6.82 [3]	6.82 [3]	6.82 [3]	6.82 [3]	6.82 [3]	6.82 [3]
2s	1.21 [3]	1.23 [3]	1.24 [3]	1.24 [3]	1.24 [3]	1.24 [3]	1.24 [3]
2p	1.19 [3]	1.21 [3]	1.22 [3]	1.22 [3]	1.21 [3]	1.22 [3]	1.22 [3]
3s	3.83 [2]	3.95 [2]	3.98 [2]	3.99 [2]	3.98 [2]	3.99 [2]	3.99 [2]
3p	3.69 [2]	3.82 [2]	3.85 [2]	3.86 [2]	3.85 [2]	3.86 [2]	3.86 [2]
3d	3.26 [2]	3.39 [2]	3.43 [2]	3.43 [2]	3.42 [2]	3.43 [2]	3.43 [2]
4s	1.41 [2]	1.50 [2]	1.52 [2]	1.52 [2]	1.52 [2]	1.52 [2]	1.52 [2]
4p	1.35 [2]	1.44 [2]	1.46 [2]	1.47 [2]	1.46 [2]	1.46 [2]	1.47 [2]
4d	1.18 [2]	1.27 [2]	1.29 [2]	1.30 [2]	1.30 [2]	1.30 [2]	1.30 [2]
4f	1.06 [2]	1.15 [2]	1.17 [2]	1.18 [2]	1.18 [2]	1.18 [2]	1.18 [2]
5s	4.49 [1]	5.06 [1]	5.21 [1]	5.23 [1]	5.25 [1]	5.23 [1]	5.23 [1]
5p	4.17 [1]	4.75 [1]	4.90 [1]	4.92 [1]	4.94 [1]	4.92 [1]	4.93 [1]
5d	3.35 [1]	3.93 [1]	4.09 [1]	4.11 [1]	4.13 [1]	4.11 [1]	4.11 [1]
5f	2.70 [1]	3.30 [1]	3.46 [1]	3.49 [1]	3.50 [1]	3.48 [1]	3.49 [1]
5g	2.20 [1]	2.85 [1]	3.01 [1]	3.04 [1]	3.06 [1]	3.04 [1]	3.05 [1]
Z_{free}	15.77	16.08	16.15	16.17	16.12	16.16	16.17
P_{total}	29.8	36.5	39.5	40.2	41.3	40.5	40.4

our calculations and experimental results [25] for zinc at zero temperature is displayed. Our calculations were performed with relativistic formulas. Our calculations usually give values a little lower than results of other authors' calculations and experiments. One of the reasons may be the local density approach to the exchange-correlation pressure, which has a large contribution at zero temperature.

C. Continuity of pressure in pressure ionization

The question of disappearance of bound levels and of the continuity of plasma properties has been studied by many authors [10–13]. Lee and Thoros [26] and More [9] considered the equation of state in the average atom model when the disappearance of bound levels leads to the appearance of resonances.

We have studied in detail the continuity of numerically calculated pressure when the pressure ionization of bound levels takes place. In our calculations reported in this subsection, we used the relativistic self-consistent approach, Eqs. (2.10)–(2.13). One of our conclusions is that one has to take into account properly the existence of narrow resonances during self-consistent calculations in order to preserve the continuity. This can be seen in the example of argon at 2.72-eV temperature and at densities

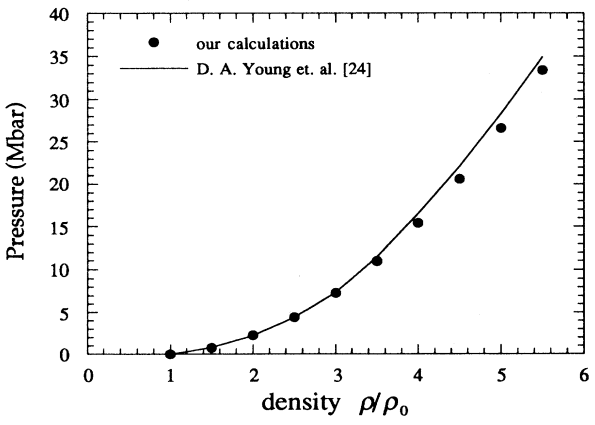

FIG. 1. Comparison of our calculations and those of Young, Wolford, and Rogers [24] for Al at zero temperature. Densities are in solid density units (2.7 g/cm^3). Our calculations were performed with relativistic corrections.

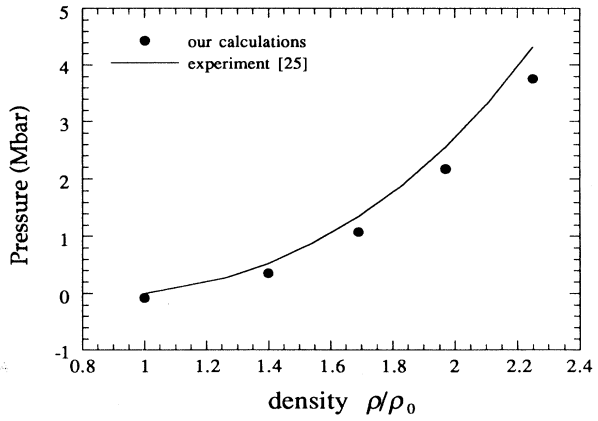

FIG. 2. Comparison of our calculations and experimental results for Zn at zero temperature. The line is based on experimental data as reduced to zero temperature by Al'tshuler, Bakanova, and Trunin [25]. Densities are in solid density units (7.1 g/cm^3). Our calculations were performed with relativistic corrections.

around $4.2\rho_0$, where ρ_0 denotes the liquid density (1.4 g/cm^3). In this case, we observe the pressure ionization of the $3p$ level. In Fig. 3, we present the phase shift δ_l and its derivative $d\delta_l/d\varepsilon$, which is proportional to the additional density of states [27], for $l=1$ as functions of energy ε in the case of density $\rho=4.21\rho_0$. This resonance has a Lorentzian shape with the peak at 2.84×10^{-3} eV and the half width of 4.5×10^{-5} eV, while the energy spectrum of free electrons which should be taken into account in density calculations extends from 0 to 10 eV. Moreover, in general, resonances become narrower with increasing l. It is therefore clear that resonances like the one shown in Fig. 3 should be searched for at each iteration and the mesh of integration with respect to energy should be chosen in order to take account of their presence.

Figure 4 shows the pressure of Ar plasma at $T=2.72$ eV as the function of atomic density. We present the results of both the cases where the presence of the resonance is and is not taken into account. The bound level $3p$ is ionized between $\rho/\rho_0=4.20$ and 4.21. This figure indicates that the calculation with a careful treatment of the resonance gives a completely continuous and smooth curve, while the one which does not take the resonance into account leads to a discontinuity at the density where the pressure ionization takes place. In Fig. 5 are presented the bound electron and free-electron contributions to the total pressure. The pressure associated with each bound level is always negative, which can be easily verified by use of Eqs. (2.15), (3.5), (3.20) and the explicit forms of the modified spherical Bessel function κ_l. From Fig. 5, we see that although both the bound electron and free-electron contributions change discontinuously when $3p$ bound level is ionized, the two discontinuities cancel each other exactly, which results in the overall continuity of the pressure.

Let us discuss this exact cancellation in more detail. In Table II, we present the contribution of each bound level to the total pressure in the case of $\rho=4.21\rho_0$. As is mentioned above, every value is negative. Table II indicates that the contributions of tightly bound levels are very

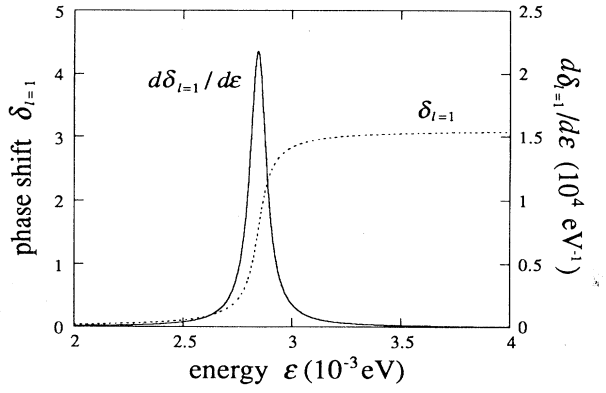

FIG. 3. Phase shift $\delta_{l=1}$ (broken line) and its derivative $d\delta_{l=1}/d\varepsilon$ for argon (Ar, $Z=1$) at $T=2.72$ eV and $\rho=4.21\rho_0$ ($\rho_0=1.4$ g/cm^3). Calculations were performed with relativistically corrected formulas.

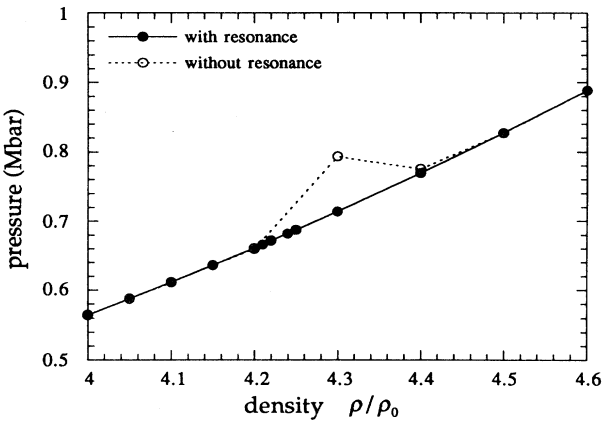

FIG. 4. Comparison of the total pressures of Ar ($T=2.72$ eV) calculated through relativistic formulas with (black circles) and without (white circles) the presence of the resonance (shown in Fig. 3) taken into account. Densities are in liquid density units (1.4 g/cm^3). The pressure ionization of $3p$ bound level takes place between $\rho=4.20\rho_0$ and $\rho=4.21\rho_0$. For densities between $\rho=4.2\rho_0$ and $\rho=4.3\rho_0$, the iteration for the self-consistent potential does not converge if the resonance is not included.

small and that those of loosely bound levels are relatively large. In particular, the contribution of $3p$ level, which is nearly ionized, is very important. When atomic density increases so that the energy eigenvalue of the $3p$ level approaches 0, the contribution of this level to the pressure does not tend to 0. In fact, the pressure of a p bound electron in the limit $\varepsilon\rightarrow-0$ is

$$P_{\text{bound } l=1}(\varepsilon\rightarrow0,\ \text{one electron}) = -\frac{3E_{\mathrm{H}}a_0^2}{\pi r_0^5}(1-\xi)f(\varepsilon=0,\mu)\ , \quad (4.1)$$

where E_{H} is the ionization potential of the hydrogen atom in the limit of infinite nuclear mass, a_0 Bohr radius, and ξ the existence probability of a p electron inside the

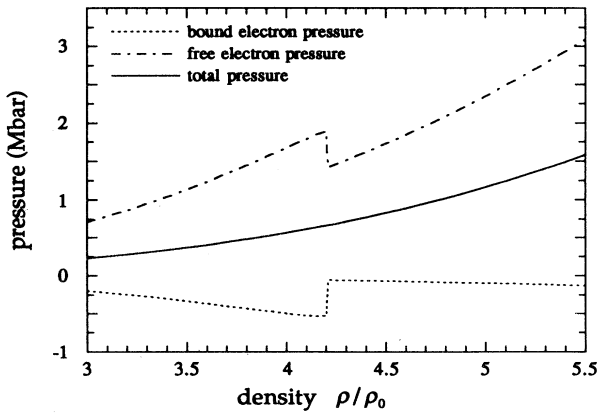

FIG. 5. Bound- and free-electron contributions to the total pressure of Ar ($T=2.72$ eV) calculated through relativistic formulas with the presence of the resonance taken into account. Densities are in liquid density units (1.4 g/cm^3).

TABLE II. The contribution of each bound level to the total pressure of Ar plasma at $T=2.72$ eV and $\rho=4.20\rho_0$.

Level	Energy (eV)	Pressure (Mbar)
$1s$	-2.87 [3]	-4.19 [-31]
$2s$	-2.67 [2]	-2.46 [-8]
$2p$	-2.20 [2]	-1.94 [-7]
$3s$	-1.08 [1]	-5.42 [-2]
$3p$	-1.20 [-2]	-4.76 [-1]

Wigner-Seitz radius in the limit $\varepsilon\rightarrow -0$. Since $0<\xi<1$, the rhs of Eq. (4.1) does not vanish. This means that when $3p$ bound electrons are ionized, the absolute value of the bound-electron contribution to the total pressure decreases discontinuously. This corresponds to the abrupt change of bound-electron pressures seen in Fig. 5. When the ionization of $3p$ level occurs, nearly six electrons disappear from the bound levels and appear in the continuum. This sudden increase of free-electron number should be absorbed by the increase of continuum density of states due to the appearance of the resonance whose parent bound level is $3p$. Unless we take into account properly the existence of the resonance during the iterations, it is not the case. This can be seen clearly in the change of chemical potential μ. Figure 6 shows chemical potential μ vs atomic density ρ/ρ_0. When calculations include the resonance properly, the chemical potential increases continuously (almost linearly) with the atomic density, while when the calculation does not take the resonance into account, the chemical potential displays a discontinuity when the pressure ionization takes place. The reason is that since the resonance is not included, the increase in the number of free electrons is not absorbed by the increase of density of states around the resonance energy but appears as an increase in the number of high-energy free electrons. This leads to the discontinuous jump of the pressure as we see in Fig. 5. On the contrary, when we take the resonance into account properly, the electrons which appear in the continuum following the pressure ionization are absorbed by the resonance. The resonance contribution to the total pressure is negative like that of bound levels, and this manifests itself in the discontinuous decrease in free-electron pressure and cancels the abrupt change of bound-electron pressure exactly as shown in Fig. 5. To sum up, narrow resonances behave very much like bound levels, physical properties like pressure and electron density changes continuously and smoothly as bound levels are ionized and pushed into the continuum, and this continuity and smoothness can be obtained in numerical calculations by taking into account properly the existence of narrow resonances at each step of iteration for atomic potential and electron density.

Figures 7 and 8 present the electron densities of argon atom at $T=2.72$ eV and $\rho=4.20\rho_0$ and $\rho=4.21\rho_0$, respectively, i.e., before and after the pressure ionization. We notice that in both cases the total density curves are almost identical and nearly constant for $r>r_0$, which is consistent with our Eqs. (2.8). There is a small deviation of electron charge density from its asymptotic value just outside the atomic sphere. Let us remark, however, that the additional charge corresponding to this deviation is very small compared with the total electronic charge contained inside the ion cell. We see that before the pressure ionization (Fig. 7) the bound-electron density extends rather far outside the Wigner-Seitz sphere. After the pressure ionization (Fig. 8) the bound-electron density at r_0 is small. This change of the bound-electron density is compensated by the free-electron density, which includes the effect of the resonance. The use of the bound wave function vanishing at infinity [Eq. (2.15)] together with the neutrality condition of the Wigner-Seitz sphere [Eqs. (2.8)] may be justified in the case of strongly coupled plasmas [7]. The usual situation will be that of Fig. 8 where the bound functions have already at r_0 their asymptotic form and are small. The case of a bound wave function which extends far outside r_0 corresponds to a situation close to pressure ionization. Due to the continuity of the

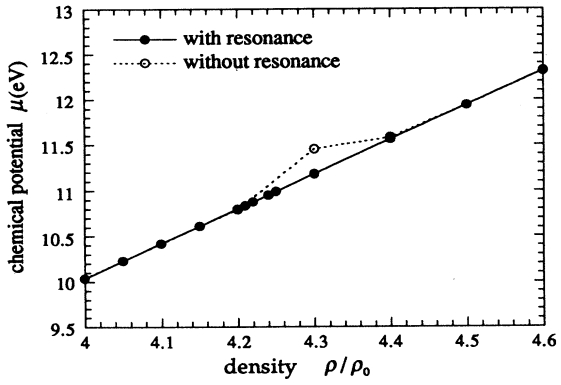

FIG. 6. Comparison of the chemical potentials of Ar ($T=2.72$ eV) calculated through relativistic formulas with (black circles) and without (white circles) the presence of the resonance taken into account. Densities are in liquid density units (1.4 g/cm^3). For densities between $\rho=4.2\rho_0$ and $4.3\rho_0$ the iteration for he self-consistent potential does not converge if the resonance is not included.

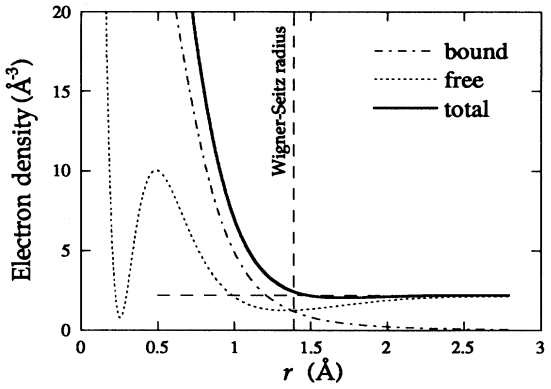

FIG. 7. The bound, free, and total electron densities of argon at $T=2.72$ eV and $\rho=4.20\rho_0$ ($\rho_0=1.4$ g/cm^3) (i.e., before the pressure ionization). The Wigner-Seitz radius equals 1.39 Å. The line corresponding to the constant asymptotic total density is prolonged inside the ion cell.

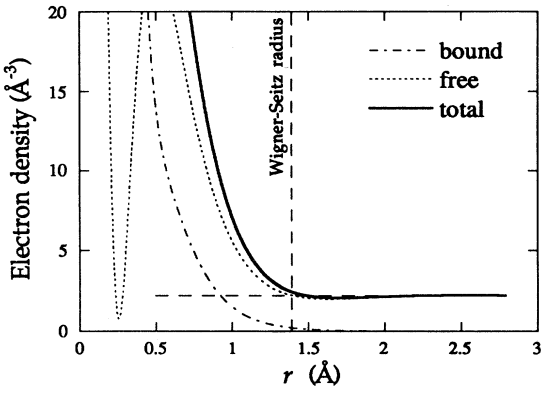

FIG. 8. The bound, free-, and total-electron densities of the argon atom at $T=2.72$ eV and $\rho=4.21\rho_0$ ($\rho_0=1.4$ g/cm^3) (i.e., after the pressure ionization). The Wigner-Seitz radius equals 1.39 Å. The line corresponding to the constant asymptotic total density is prolonged inside the ion cell.

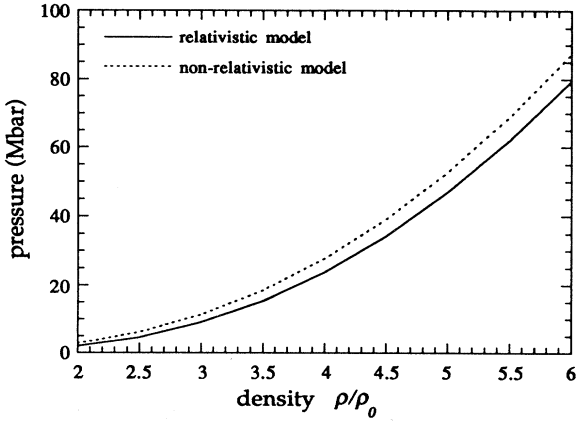

FIG. 9. Comparison of relativistic and nonrelativistic calculations of pressure for Hg ($Z=80$) at $T=2.72$ eV. Densities are in liquid density units (13.6 g/cm^3).

total density (Figs. 7 and 8) the model works also in that case.

D. Effects of relativistic corrections to bound- and free-electron states

Relativistic effects on bound-energy levels and radial wave functions become important for high-Z elements [19]. In Sec. B, we have derived the relativistic pressure formula in the Pauli approximation. The difference with respect to the nonrelativistic approach is the presence of the correction $(1+\varepsilon/2E_0)^{-1}$ and the fact that the one-electron states and chemical potential in the formulas Eqs. (3.18)–(3.21) are calculated from the relativistically corrected wave equation, Eq. (2.10). Figure 9 presents pressure versus density of Hg ($Z=80$) at $T=2.72$ eV. We show the results of both relativistic and nonrelativistic calculations. From this figure, we see that in this case relativistic effects are non-negligible and that relativistic corrections should, in principle, be included in calculations for high-Z elements.

On the other hand, the relativistic corrections are expected to be relatively small in the case of low and intermediate-Z elements and not too high temperatures. We will show the results of both relativistic and nonrelativistic calculations in the case of argon ($Z=18$) at $T=2.72$ eV.

In the spherical ion-cell calculations, sometimes bound- and free-electron densities are evaluated through different expressions. Our results, however, indicate that both bound and free electrons should be treated in the same manner, i.e., that one should treat both simultaneously either in the relativistic or in the nonrelativistic way. In principle, one may reason that only low lying bound energy levels are affected by relativistic corrections and that, therefore, the relativistic treatment of bound levels combined with the nonrelativistic approximation for free electrons may be sufficient. We will show that this is not the case from the viewpoint of the continuity of plasma pressure. In Fig. 10, we display pressure versus density of argon at 2.72-eV temperature. The results of three calculations are shown: (i) relativistic treatment of all electrons, (ii) nonrelativistic treatment of all electrons, (iii) relativistic treatment of bound electrons and nonrelativistic treatment of free electrons. As one could expect, the difference between the results of (i) and (ii) is small. The mixed case (iii) leads, however, to the presence of a dip in the pressure curve at the value of the density for which pressure ionization takes place. We have studied the origin of this dip. Table III presents one-electron energy levels and pressures obtained in each of the three cases at the density $4.05\rho_0$. These results indicate that the relativistic effects on tightly bound levels are relatively more important, as expected, but that the contributions of these levels to the total pressure are so small that they cannot affect the total pressure. On the other hand, the change in the pressure of loosely bound levels introduced by relativistic corrections is not large enough to explain the dip seen in Fig. 10. We have found that the

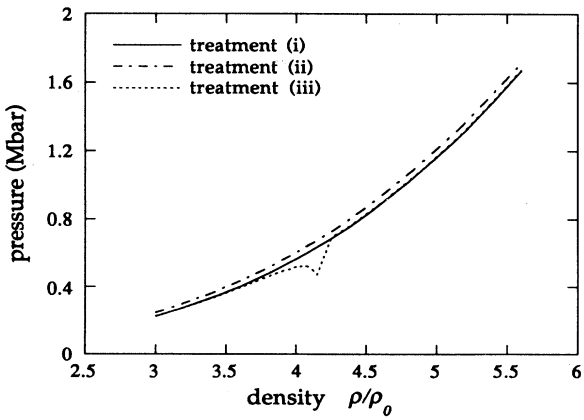

FIG. 10. Comparison of the total pressures of Ar ($T=2.72$ eV) calculated for the cases (i)–(iii) described in the text, with the presence of the resonance taken into account. Densities are in liquid density units (1.4 g/cm^3).

TABLE III. The one-electron energy and the pressure of each bound level of Ar plasma at $T=2.72$ eV and $\rho=4.05\rho_0$ in each of the cases (i)–(iii) described in the text. Energies are in eV, and pressures are in Mbar.

	Case (i)		Case (ii)		Case (iii)	
Level	Energy	Pressure	Energy	Pressure	Energy	Pressure
$1s$	−2.87 [3]	−1.57 [−31]	−3.08 [3]	−8.28 [−33]	−2.87 [3]	−1.57 [−31]
$2s$	−2.67 [2]	−1.75 [−8]	−2.82 [2]	−9.63 [−9]	−2.67 [2]	−1.76 [−8]
$2p$	−2.21 [2]	−1.41 [−7]	−2.18 [2]	−1.61 [−7]	−2.21 [2]	−1.41 [−7]
$3s$	−1.12 [1]	−4.78 [−2]	−1.26 [1]	−4.11 [−2]	−1.12 [1]	−4.78 [−2]
$3p$	−2.58 [−1]	−4.65 [−1]	−4.59 [−2]	−4.57 [−1]	−2.64 [−1]	−4.65 [−1]

origin of the dip is a slight change of the $3p$ wave function in method (iii) with respect to the result of method (ii). The $3p$ wave functions obtained in each of the cases (i)–(iii) are displayed on Fig. 11. The integral $\int_0^{r_0} y_{3p}^2(r)dr$ equals 0.700, 0.634, and 0.701 for cases (i), (ii), and (iii), respectively. Since $2(2l+1)=6$ for the $3p$ level, the total number of bound electrons in case (ii) is lower by the number $0.40\times$(Fermi-Dirac factor) than the number of bound electrons in cases (i) and (iii). This fact and the neutrality of the ion-sphere lead in turn to a difference in the number of free electrons [2.00 for (i), 2.37 for (ii), and 2.01 for (iii)]. Although this difference seems to be small, it concerns essentially the high-energy free electrons, which have important contributions to the pressure. Thus, finally, the pressure in case (iii) is much lower than in case (ii) and this effect explains the dip seen in Fig. 10. In case (i), in spite of the fact that the free-electron number is lower than in case (ii), the continuity of pressure is preserved due to the relativistic corrections to free-electron states. From Fig. 10, we see that cases (i) and (iii) give practically the same result except for the dip. Thus, for densities far from the value where pressure ionization occurs, i.e., where there are no very loosely bound levels, the relativistic corrections affect only tightly bound levels which do not have much impact on pressure.

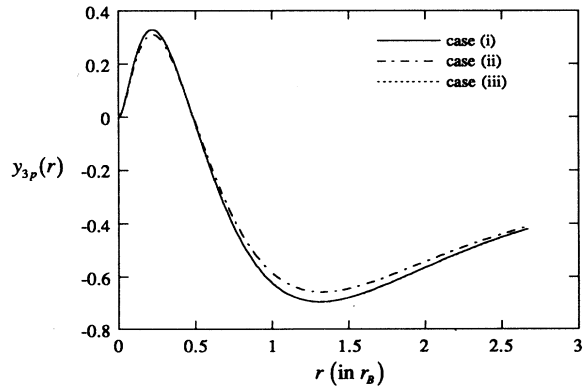

FIG. 11. Comparison of the radial wave functions $y_{3p}(r)$ of the $3p$ bound level of Ar ($T=2.72$ eV, $\rho=4.05\rho_0$) calculated for the cases (i)–(iii) described in the text, with the presence of the resonance taken into account. The distance from the nucleus, r, is in Bohr radius. The curves corresponding to the cases (i) and (iii) almost overlap.

The dip in case (iii) can be considered as an artifact due to the notion of the neutral Wigner-Seitz ion sphere. It is, however, important to note that when one uses exactly the same one-electron Hamiltonian for both bound and free electrons, calculated pressure preserves its continuity [cases (i) and (ii)]. Similar effects may be encountered in calculations of other quantities such as partition function or opacity. This observation stresses the need of a consistent description of bound and free electrons in the self-consistent-field spherical ion-cell model.

V. CONCLUSIONS

We have studied the pressure ionization and the continuity of pressure calculated via the quantum-mechanical formulas in the self-consistent-field spherical ion-cell model for partially ionized plasma. It appears that self-consistent calculations of electron density and atomic potential are correct only when a careful search for narrow resonances is performed at each iteration. In that case, pressure-versus-density curves are continuous and smooth despite pressure ionization phenomena.

We derived a relativistic pressure formula in the Pauli approximation. This formula is only slightly different from the nonrelativistic one. Our results indicate that bound and free electrons should be treated in the same manner, i.e., both with relativistic corrections or both without them. These observations concern all the self-consistent-field calculations which use spherical and neutral atomic cells of finite size, since the existence of narrow continuum resonances is a common feature of finite-range potentials.

ACKNOWLEDGMENTS

Discussions with F. Grimaldi are gratefully acknowledged. This research has been partially supported by Swiss Federal Office for Science and Education, "Union des Centrales Suisses d'Electricité" and Swiss National Science Fund.

APPENDIX A: THE FORM OF U_A IN THE PAULI THEORY FOR A CENTRAL FIELD

In the Pauli theory for a central field [18], the large components U_A of Dirac spinor are simultaneous eigen-

states of the operators $\mathbf{J}^2$, $\mathbf{J}_z$, $\mathbf{L}^2$, $\mathbf{s}^2$, and $2\mathbf{L}\cdot\mathbf{s}$. For given values of ε (or n) and l, there are $(2l+1)$ eigenstates, which are classified in two by the quantum number j and the eigenvalue X of $2\mathbf{L}\cdot\mathbf{s}$, each labeled $+$ and $-$, respectively, as follows,

$$\begin{aligned} j_+ &= l+\tfrac{1}{2}\ , \quad X_+ = l\ , \\ j_- &= l-\tfrac{1}{2}\ , \quad X_- = -(l+1)\ , \end{aligned} \tag{A1}$$

and there are $(2l+1)$ states for $+$ and $2l$ states for $-$ with normalized eigenfunctions,

$$\begin{aligned} U_{A+,l,j_z=m+1/2} &= \frac{1}{\sqrt{2l+1}}\frac{y_{+,l}(r)}{r}\begin{bmatrix} \sqrt{l+m+1}\,Y_{l,m}(\theta,\varphi) \\ -\sqrt{l-m}\,Y_{l,m+1}(\theta,\varphi)\end{bmatrix}, \quad m=-l-1,-l,\ldots,l\ , \\ U_{A-,l,j_z=m+1/2} &= \frac{1}{\sqrt{2l+1}}\frac{y_{-,l}(r)}{r}\begin{bmatrix} \sqrt{l-m}\,Y_{l,m}(\theta,\varphi) \\ \sqrt{l+m+1}\,Y_{l,m+1}(\theta,\varphi)\end{bmatrix}, \quad m=-l,-l+1,\ldots,l-1\ , \end{aligned} \tag{A2}$$

where we set $Y_{l,l+1}(\theta,\varphi)=Y_{l,-l-1}(\theta,\varphi)\equiv 0$, and the radial wave functions $y_{\pm,l}(r)$ are calculated from Eq. (2.10). Let us assume that these $2(2l+1)$ states are occupied by electrons with equal probability. Then the average value of X is

$$\bar{X}=\frac{(2l+2)l+2l(-l-1)}{2(2l+1)}=0\ . \tag{A3}$$

The use of Eq. (A2) makes us find

$$\begin{aligned} \sum_{\pm m} U_A^+ U_A &= \sum_{m=-l-1}^{l} U_{A+}^+ U_{A+} + \sum_{m=-1}^{l-1} U_{A-}^+ U_{A-} \\ &= \frac{2(l+1)}{4\pi}\frac{y_{+,l}^2(r)}{r^2}+\frac{2l}{4\pi}\frac{y_{-,l}^2(r)}{r^2}\ , \end{aligned} \tag{A4}$$

$$\sum_{\pm m} X U_A^+ U_A = \frac{2l(l+1)}{4\pi r^2}[y_{+,l}^2(r)-y_{-,l}^2(r)]\ , \tag{A5}$$

where we have used the identity $\sum_{m=-l}^{l}|Y_{lm}(\theta,\varphi)|^2=(2l+1)/4\pi$ [18]. Equation (A4) indicates that the electron number density is independent of the angular directions (θ,φ) as well as in the nonrelativistic treatment. In the present study, we set $V_{so}=0$ in Eq. (2.10) as is mentioned in subsection II B. It follows then that $y_{+,l}(r)=y_{-,l}(r)=y_l(r)$, and, therefore, Eqs. (A4) and (A5) become

$$\sum_{\pm,m} U_A^+ U_A = \frac{2(2l+1)}{4\pi}\frac{y_l^2(r)}{r^2}\ , \tag{A6}$$

$$\sum_{\pm,m} X U_A^+ U_A = 0\ . \tag{A7}$$

Equation (A6) leads to Eqs. (2.19) and (2.20).

APPENDIX B: PROOF OF EQ. (3.24)

In order to derive Eq. (3.24), we first prove the following identity:

$$-\sum_{l=0}^{\infty}(2l+1)j_l(x)j_l'^1(x)=\sum_{l=0}^{\infty}(2l+1)j_l'^2(x)=\tfrac{1}{3}\ . \tag{B1}$$

The first equality of the previous identity is easy to obtain. By differentiating the well-known identity $\sum_{l=0}^{\infty}(2l+1)j_l^2(x)=1$ [20] twice with respect to x, we get

$$2\sum_{l=0}^{\infty}(2l+1)[j_l'^2(x)+j_l(x)j_l'^1(x)]=0\ , \tag{B2}$$

which immediately leads to the first equality of Eq. (B1). To prove the second equality of Eq. (B1), we start with the identity [20]

$$e^{ix\cos\theta}=\sum_{l=0}^{\infty}(2l+1)i^l j_l(x)P_l(\cos\theta)\ , \tag{B3}$$

where P_l is a Legendre polynomial, which satisfies the following relation:

$$\int_0^1 P_l(z)P_{l'}(z)dz=\frac{2}{2l+1}\delta_{ll'}\ . \tag{B4}$$

By differentiating (B3) with respect to x, we get

$$i\cos(\theta)e^{ix\cos\theta}=\sum_{l=0}^{\infty}(2l+1)i^l j_l'(x)P_l(\cos\theta)\ . \tag{B5}$$

If we multiply each side of Eq. (B5) by its complex conjugate and replace $\cos\theta$ by z, we get

$$z^2=\sum_{l=0}^{\infty}\sum_{l'=0}^{\infty}(2l+1)(2l'+1) \times j_l'(x)j_{l'}'(x)P_l(z)P_{l'}(z)\ , \quad -1\le z\le 1\ . \tag{B6}$$

The integration of the previous equation with respect to z from -1 to 1 and the use of Eq. (B4) lead us to the second equality of Eq. (B1).

Now we prove Eq. (3.24) for the nonrelativistic treatment. The formula for the relativistic treatment can be proved in the same way. It is more convenient to start with the expression of $\Pi_{k,l}(y_{0;\varepsilon,l})$ obtained directly from Eq. (3.3):

$$\Pi_{k,l}(y_{0;\varepsilon,l})=\frac{\hbar^2}{2m}\frac{2(2l+1)}{4\pi} \times\left[\left[\frac{d}{dr}\frac{y_{0;\varepsilon,l}}{r}\right]^2 -\frac{y_{\varepsilon,l}}{r}\frac{d^2}{dr^2}\left[\frac{y_{0;\varepsilon,l}}{r}\right]\right]_{r=r_0}\ , \tag{B7}$$

rather than to start with Eq. (3.7). By setting $\delta_{\varepsilon,l}=0$ in Eq. (2.17), we get the expression of $y_{0;\varepsilon,l}(r)$:

$$y_{0;\varepsilon,l}(r)=\left[\frac{2m}{\hbar^2}\frac{k}{\pi}\right]^{1/2} r j_l(kr) \ . \tag{B8}$$

If we substitute the previous equation into Eq. (B7), we obtain

$$\Pi_{k,l}(y_{0;\varepsilon,l})=\frac{(2l+1)k^3}{2\pi^2}[j_l'^2(kr_0)-j_l(kr_0)j_l''(kr_0)] \ . \tag{B9}$$

By using Eqs. (B1) and (B9), we finally obtain Eq. (3.24) for the nonrelativistic model.

[1] D. A. Liberman, Phys. Rev. B **20**, 4981 (1979).
[2] D. A. Liberman, J. Quant. Spectrosc. Radiat. Transfer **27**, 335 (1982).
[3] F. Perrot, Phys. Rev. E **47**, 570 (1993).
[4] B. F. Rozsnyai, Phys. Rev. A **5**, 1137 (1972).
[5] B. F. Rozsnyai, Phys. Rev. A **43**, 3035 (1991).
[6] J. Davis and M. Blaha, J. Quant. Spectrosc. Radiat. Transfer **27**, 307 (1982).
[7] M. W. C. Dharma-wardana and F. Perrot, Phys. Rev. A **26**, 2096 (1982).
[8] T. D. Beynon and D. K. K. Landeg, J. Quant. Spectrosc. Radiat. Transfer **44**, 129 (1990).
[9] R. M. More, Adv. At. Mol. Phys. **21**, 305 (1985).
[10] W. Kohn and C. Majumdar, Phys. Rev. **138**, A1617 (1965).
[11] A. G. Petschek, Phys. Lett. **34A**, 411 (1971).
[12] A. G. Petschek and H. Cohen, Phys. Rev. A **5**, 383 (1972).
[13] W. Ebeling, W. D. Kraeft, and D. Kremp, *Theory of Bound States and Ionization Equilibrium in Plasmas and Solids* (Akademie-Verlag, Berlin 1976).
[14] G. M. Gandel'man, Zh. Eksp. Teor. Fiz. **43**, 131 (1962) [Sov. Phys. JETP **16**, 94 (1963)].
[15] T. Blenski and J. Ligou, Comput. Phys. Commun. **50**, 303 (1988).
[16] F. Perrot and M. W. C. Dharma-wardana, Phys. Rev. A **30**, 2619 (1984).
[17] H. Iyetomi and S. Ichimaru, Phys. Rev. A **34**, 433 (1986).
[18] H. A. Bethe and E. E. Salpeter, *Quantum Mechanics of One- and Two-Electron Atoms* (Springer-Verlag, Berlin, 1957).
[19] R. D. Cowan, *The Theory of Atomic Structure and Spectra* (University of California Press, Berkeley, 1981).
[20] M. Abramowitz and I. A. Stegun, *Handbook of Mathematical Functions,* Ninth Printing (U.S. GPO, Washington, DC, 1970).
[21] C. Bruderer, *Travail de Diplôme* (EPEL, Lausanne, 1991).
[22] W. Pauli, Handb. Phys. **5**, 1 (1958).
[23] A. Messiah, *Quantum Mechanics* (North-Holland, Amsterdam, 1965).
[24] D. A. Young, J. K. Wolford, and F. J. Rogers, Phys. Lett. **108A**, 157 (1985).
[25] L. V. Al'tshuler, A. A. Bakanova, and R. F. Trunin, Zh. Eksp. Teor. Fiz. **42**, 91 (1962) [Sov. Phys. JETP **15**, 65 (1962)].
[26] C. M. Lee and E. I. Thorsos, Phys. Rev. A **17**, 2073 (1978).
[27] P. W. Anderson and W. L. McMillan, in *Theory of Magnetism in Transition Metals,* Proceedings of the International School of Physics "Enrico Fermi," Course XXXVII, Varenna, 1966, edited by W. Marshall (Academic Press, New York, 1967).